# What does non-exponential diffusion-weighted signal decay reveal about myocellular barriers?

John G Georgiadis[1,2], Caroline G Tennyson[1], Danchin D Chen[1], Armen A Gharibans[1], and Curtis L Johnson[1,2]

[1]*Mechanical Science and Engineering, University of Illinois at Urbana-Champaign, Urbana, IL, United States,* [2]*Beckman Institute, University of Illinois at Urbana-Champaign, Urbana, IL, United States*

## INTRODUCTION

Diffusion Tensor Imaging (DTI) has been increasingly employed to assess muscle quality in older adults *in vivo* [1,2]. In addition to improved MR sequences, the DTI encoding parameters have to be selected judiciously in order to ensure high SNR and fidelity in muscle fiber tract reconstruction [1,3]. Towards this objective, computer simulations [4] and analysis coupled with experiments on human calf muscle [5] have focused on the effect of intramuscular fat on muscle DTI parameters as a function of b-value. A recent simulation of diffusion-weighted signal decay based on pure isotropic Gaussian diffusion and coupled with human calf muscle experiments has addressed the effect of encoding parameters, (simulated) SNR, and muscle $T_2$ on the computation of the DTI metrics [3]. However, it is well accepted that the DTI tensor is anisotropic in all three principal directions, which indicates that intra- and inter-cellular barriers restrict water diffusion in the muscle [6, 7]. The aim of this work is to explore this effect on the diffusion-weighted signal by extending an anisotropic myofiber model [7].

## METHODS

***Experiment***: 30-direction DTI data were collected over 7 contiguous axial slices using a twice-refocused spin-echo sequence with a single-shot EPI readout on a Siemens Trio 3T scanner. The subject (51 year-old non-sedentary man) was oriented in a feet-first supine position and data were acquired using a combination of an eight-channel spine coil and a flexible body matrix surface coil positioned over the left thigh. DTI sequence parameters included: TR/TE=3000/79 ms, FOV=250×250mm$^2$, matrix size = 76×76, slice thickness=10mm, b=300 to 1000s/mm$^2$ in increments of 50s/mm$^2$, and Nex=5. Parallel imaging was enabled with an acceleration factor of 2 to reduce scan time and reduce magnetic susceptibility artifacts. Corresponding high-resolution $T_2$-weighted anatomical images were also taken at each slice to aid in segmentation of muscles. ***Simulation:*** The signal from a diffusion-weighted sequence applied on a two-compartment model consisting of a periodic array of fibers was simulated. This model mimics a periodic array of myofibers surrounded by a uniform matrix representing the endomysium, and with the sarcolemma represented by a partially permeable diffusion barrier. We have developed a numerical code based on an accurate boundary condition implementation of the Lattice Boltzmann scheme [8] to integrate the Bloch-Torrey partial differential equation in 2-D.

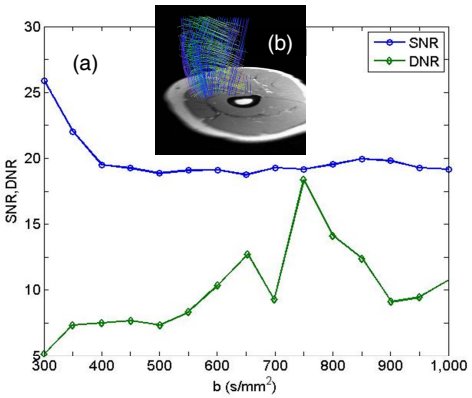


**Fig 1. (a)** Experimental signal-to-noise (SNR) and diffusion-to-noise (DNR) ratios. **(b)** Primary (blue) and secondary (green) diffusion tensor lines for the middle section of the *vastus medialis*.

## RESULTS

A rectangular ROI was placed in the *vastus medialis* region on each axial slice. Quantitative data analysis included calculation of the DTI metrics (eigenvalues), as well as SNR and DNR, all averaged over the ROI, cf. Fig 1(a). The DNR, defined as the SNR of the calculated diffusion tensor trace map, is mostly independent of experimental parameters [9]. Fiber tractography and visualization was performed using the Diffusion Toolkit and TrackVis, cf. Fig 1(b). The Bloch-Torrey equation was solved in the plane (x,y) normal to the myofiber axis, in order to simulate $\ln(S/S_0)$ for two periodic arrays, one with elliptical and the other with circular cross section, cf. Fig 2. A sarcolemma permeability value of 13 μm/s was assumed, and the remaining parameters for the intra- and extra-cellular compartments used in [7] were adopted. Both experiment and simulation reveal non-exponential signal decay with b-value. The maxima (denoted by arrows in Fig. 2) correspond to $q^{-1}$=83 μm and $q^{-1}$=52 μm for simulation and experiment, respectively, where q is the reciprocal displacement.

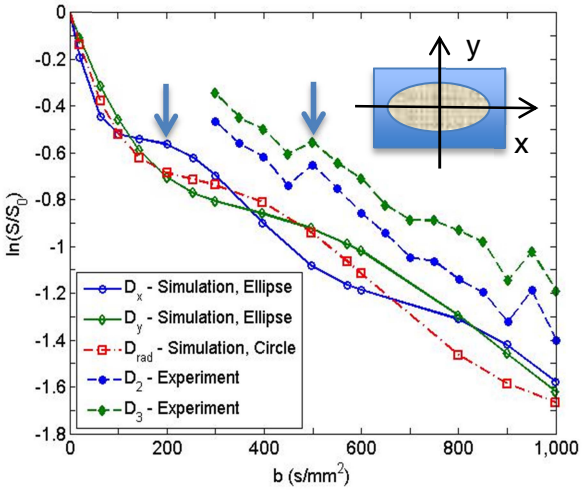


**Fig 2.** Diffusion-weighted signal decay from simulation (solid lines) and experiment (dash lines) as a function of b-value. The secondary and tertiary eigenvalues of the diffusion tensor ($D_2$, $D_3$) correspond to the primary and secondary eigenvalues for the myofiber elliptical cross section ($D_x$, $D_y$) with dimensions 94 μm and 66 μm. $D_{rad}$ marks the simulation for a circular cross section of diameter 76 μm.

## DISCUSSION AND CONCLUSION

Although it varies from slice to slice (not shown here), the SNR vs b-value curve plotted in Fig 1 is consistent with other analytical models [5]. Note that SNR ~20 which is close to the minimum level required for accurate muscle DTI [3]. The measured DNR vs b behavior does not vary from slice to slice, and its maximum in Fig 1 suggests an optimum b value of 750 s/mm$^2$. The non-exponential diffusion-weighted signal decay with b shown in Fig 2 indicates the detection of water diffusion barriers with interstitial spacing of 52-83 μm. These values are consistent with the long TE employed here, as well as reported diameters and packing densities of myofibers in the *vastus medialis* [10]. Unlike the measured signal decay, the maxima in the simulated signal decay for diffusion along x and y do not coincide. Our simulation results, obtained with a continuum two-compartment model, bolster the view that the diffusion-weighted signal from large cells, such as muscle fibers, cannot be interpreted with lumped two-compartment models, such as the Kärger model [11]. On the other hand, our results indicate that the idealized (elliptical) cross-sectional geometry of the sarcolemma could not account for the fact that $D_2$ and $D_3$ differ, and suggest the need to introduce some level of anisotropic myocellular compartmentalization in the myofiber model [7].

**REFERENCES:** [1] Gharibans AA et al., *Proc ISMRM* 19, 2011. 273; [2] Gharibans AA et al., *Proc ISMRM* 20, 2012. 1426; [3] Froeling M et al. *NMR Biomed* 26: 1339-52, 2013; [4] Damon BM, *MRM* 60(4):934-944, 2008; [5] Karampinos DC et al. *NMR Biomed* 25(5): 766-778, 2012; [6] Galban, CJ et al. *Eur J Appl Physiol* 93: 253-262, 2004; [7] Karampinos DC et al., *Ann Biomed Eng* 37: 2532-46, 2009; [8] Li L et al. *J Comp Phys* 237:366-395, 2013; [9] Armitage PA & Bastin ME, *MRM* 45: 1056–1065, 2001; [10] Travnik L et al. *J Anatomy* 187:403-411, 1995; [11] Fieremans E et al. *NMR Biomed* 23: 711-724, 2010.